American Mineralogist, Volume 76, pages 1120–1133, 1991

Mechanisms and kinetics of Al-Si ordering in anorthite: II. Energetics and a Ginzburg-Landau rate law

Michael A. Carpenter
Department of Earth Sciences, University of Cambridge, Downing Street, Cambridge CB2 3EQ, England

Abstract

A suite of synthetic anorthite crystals with different states of Al-Si order, from $C\bar{1}$ with short-range order through incommensurately ordered to commensurately ordered with the thermodynamically stable $I\bar{1}$ ordering scheme, have been used for lattice parameter and high-temperature solution calorimeter measurements. The macroscopic order parameter, Q_{od}, describing the degree of order with respect to the $C\bar{1} \rightleftharpoons I\bar{1}$ transition, has been followed through its relationship with the spontaneous strain, ϵ_s ($\epsilon_s \propto Q_{od}^2$). To a first approximation, the excess enthalpy due to ordering is linear with Q_{od}^2, giving a minimum value of $-3.3 \pm \sim 1$ kcal/mol for the enthalpy of the exchange reaction (-Al-O-Al-) + (-Si-O-Si-) → 2(-Al-O-Si-). Both the strain and enthalpy data show that, for a limited range of Q_{od}, the kinetics of ordering can be described by an empirical rate law of the form

$$\frac{Q_{od}^2}{AR(T - T_c)} = \ln t - \frac{\Delta H^*}{RT} + \frac{\Delta S^*}{R} - \ln \tau_0.$$

Values of $A = -2.1 \times 10^{-5}$, $T_c = 2215$ °C, $\Delta H^* = 124 \pm \sim 15$ kcal/mol, and $\tau_0 \cdot \exp(-\Delta S^*/R) = 9 \times 10^{-21}$ s were obtained. This type of rate law can be understood in terms of solutions to the Ginzburg-Landau rate equation for systems in which the degree of order is inhomogeneous on a local scale.

Type b antiphase domains (APDs) in the more ordered samples have been characterized by transmission electron microscopy, allowing the relationship between excess enthalpy and APD size, δ, to be determined. Treating the boundaries between APDs as surfaces yields defect energies of $1.22 \pm \sim 0.30 \times 10^{-5}$, $0.94 \pm \sim 0.20 \times 10^{-5}$, and $0.67 \pm \sim 0.20 \times 10^{-5}$ cal·cm^{-2} for crystals annealed at 1400, 1300, and 1200 °C, respectively. The apparent decrease in these defect energies with decreasing temperature suggests that the antiphase boundaries are stabilized by Al-Si ordering on the basis of their local $C\bar{1}$ symmetry. They might even become stable features of the crystals at some low temperature, with implications for the nature of periodic antiphase boundaries in the intermediate plagioclase structure.

Introduction

In the first paper of this series (Carpenter, 1991a), it was shown that anorthite crystals prepared from glass develop a metastable incommensurate superstructure as progressive Al-Si ordering, from an initially disordered or short-range ordered ($C\bar{1}$) state, takes place toward the equilibrium ordered ($I\bar{1}$) state. The nature of the ordering sequence was characterized mainly by electron diffraction. In this paper, the results of enthalpy and spontaneous strain measurements for the same sequence of structural states are presented. The kinetics of ordering are then analyzed on the basis of solutions to the Ginzburg-Landau (GL) rate equation. An essential link between the different measurements is provided by a macroscopic order parameter, Q_{od}, and its relationship with a short-range order parameter, σ, which may in turn be defined in terms of the number of Al-O-Al linkages present in the synthetic anorthite crystals.

Applications of the GL rate equation to order-disorder processes in minerals have been set out in some detail by Salje (1988, 1989), Salje and Wruck (1988), and Carpenter and Salje (1989). Behind the whole approach is the concept that changes in the properties of a crystal resulting from a phase transition may be defined explicitly for both equilibrium and nonequilibrium conditions by using a common order parameter, Q. For a continuous transition, the variation of Q with time may be proportional to the variation of free energy with Q. In effect, the kinetic pathway is across a particular free energy surface, which can be understood using thermodynamic parameters derived from equilibrium data. If the equilibrium properties are known, it may be possible to reproduce the kinetic behavior exactly by integration of the GL equation, but if they are not, many approximate solutions, valid for specific conditions, may still be derived from the generalized rate law. One important factor in this context is

0003–004X/91/0708–1120$02.00

the role of fluctuations, and a distinction can be drawn between systems that remain fully homogeneous with respect to Q and systems that develop local inhomogeneities. In the former, the kinetic pathway is through states that may also occur under some equilibrium conditions, as appears to be the case for cation disordering in omphacite (Carpenter et al., 1990a, 1990b); in the latter, additional gradient energy terms may be required.

The electron optical observations set out in Carpenter (1991a) show that Al-Si ordering in anorthite prepared from glass does not proceed by the evolution of a single homogeneous order parameter. The nature of the modulated structure and its thermodynamic properties are not, as yet, sufficiently well known to allow numerical integration of the GL equation. For the time being, therefore, it has been necessary to adopt an empirical approach to the kinetic analysis. The enthalpy and strain data are used to fit an approximate rate law for Q_{od}, which is then interpreted in terms of the factors that should be treated explicitly in a GL solution. Some preliminary results have already been mentioned briefly by Carpenter (1988) and Carpenter and Salje (1989).

Experimental methods

The anorthite synthesis procedure, using ~2 mm cubes of glass as starting material, has been described in Carpenter (1991a). A few of the crystallized cubes were set aside for other observations, but the majority were crushed in an agate mortar and pestle and separated into size fractions using 45 μm and 150 μm sieves. The finest fraction, which passed through the 45 μm sieve, was used for X-ray powder diffraction, and the fraction in the nominal size range 45–150 μm was used for solution calorimetry.

Calorimetric data were obtained using a high-temperature solution calorimeter (Calvet type) that was built in Cambridge to the design specifications of A. Navrotsky (e.g., see Navrotsky, 1977). The thermopile signal was measured with a Kiethley 181 nanovoltmeter and recorded in a BBC microcomputer. Lead borate ($Pb_2B_2O_5$) at 700 °C was used as the flux, and conventional calibration procedures, as described for example by Carpenter et al. (1983, 1985), were followed. For each synthetic anorthite sample, 5–8 heat of solution values were determined, using ~30 mg batches of powder. A stirring correction, obtained using clean, empty sample holders, was applied to each heat of solution measurement. Scatter in the data, i.e., $\pm 1\sigma$ for ca. five experiments, was on the same scale as reported for natural plagioclase samples by Carpenter et al. (1985), suggesting that the performance of the Cambridge calorimeter is comparable to the calorimeter of A. Navrotsky (originally at Arizona State University, now at Princeton University). Absolute values for the heat of solution (ΔH_{soln}) for a given sample need not be the same from different calorimeters because of other variables such as the exact composition of the lead borate flux.

Lattice parameters were refined from X-ray powder diffraction data obtained with a focusing Guinier camera and monochromatized Cu$K\alpha_1$ radiation. Si was used as an internal standard, and films were exposed for 2 or 3 d in a vacuum to optimize signal to background ratios. Individual lines were indexed using the data of the calculated powder pattern for anorthite given by Borg and Smith (1969). Up to 50 reflections were used for the refinements in a least-squares refinement program based on the method of Burnham (1962). The powder patterns from samples annealed for relatively short times at 1100 and 1200 °C typically had broader and weaker lines than patterns from the other samples, and only 35–40 lines could be measured reliably from these films. As a consequence, the standard deviations of the final refined lattice parameters are slightly larger than average. At least some of the line broadening is probably because of the submicroscopic twinning described in Carpenter (1991a).

Values of ΔH_{soln} for all the synthetic anorthite samples are given in Table 1, along with complete details of the heat treatments and the observations made by transmission electron microscopy. Lattice parameters are given in Table 2. Two samples, ANC62 and ANC71, received two heat treatments, ~14–16 d at 1400 °C followed by a prolonged period at 1300 and 1200 °C, respectively.

Strain analysis

A scalar spontaneous strain, ϵ_s, which is related to the order parameter, Q_{od}, for the $C\bar{1} \rightleftharpoons I\bar{1}$ transition in anorthite, may be calculated from the room-temperature lattice parameters given in Table 2. The procedure for this has been set out in detail by Carpenter et al. (1990c) and is only summarized here. First, the reference state for which ϵ_s is defined as zero has been assumed to be the synthetic anorthite with the smallest value of γ yet obtained (ANC19, 15 min at 1100 °C). This sample contained some relict glass, and the crystalline fraction gave extremely diffuse and barely detectable e reflections and streaked c reflections in overexposed electron diffraction patterns. Since the reference state and all the more ordered states are triclinic, there are no symmetry constraints on the six elements, x_1–x_6, which make up the spontaneous strain tensor. Values of x_1–x_6, calculated using the equations given by Carpenter et al. (1990c) and Redfern and Salje (1987), are plotted as a function of the logarithm of annealing time, t, in Figure 1. It is apparent that although all the strain elements are small, x_6 is large relative to x_1–x_5; x_6 depends principally on cos γ and is the parameter which is expected to be the most sensitive to changes in Al-Si order in feldspars (Salje et al., 1985; Carpenter, 1988).

The diagonalized strain matrix gives three principal strains, ϵ_1, ϵ_2, and ϵ_3, which represent the linear strains along orthogonal axes. The magnitudes of ϵ_1–ϵ_3 are shown as a function of ln t in Figure 2, and their orientations with respect to the feldspar lattice are shown in Figure 3. The magnitude of ϵ_2 is close to zero, whereas ϵ_1 and ϵ_3 are approximately equal but opposite in sign, which means that the character of the distortions accompanying Al-Si ordering is almost pure shear. The plane of shearing is

TABLE 1. Heat treatments, product characterization by transmission electron microscopy, and strain and calorimetric data for anorthite synthesized from glass

Sample no.	Heat treatment		TEM characterization of product				Scalar strain	Calorimetry	
	T (°C)	t (h)	e/b	$\|2\mathbf{s}\|^{-1}$ (Å)	$\mathbf{b}^* \wedge \mathbf{s}$ (°)	b domain size (Å)	ϵ_s ($\pm 1\ \sigma$)	ΔH_{soln} (kcal/mol, $\pm 1\sigma$)	No. of measurements
ANC10*	1376 ± 2	0.017	e	29**	80**				
ANC32	1390 ± 5	0.017	e	28 ± 1	76 ± 2		0.0037(2)	13.10 ± 0.19	6
ANC60	1385 ± 5	0.017	e	30 ± 1	78 ± 3		0.0039(2)	13.20 ± 0.15	6
ANC11*	1383 ± 12	0.067					0.0045(3)	13.54 ± 0.20	4
ANC33	1392 ± 8	0.067	e	42, 46	60, 75		0.0047(2)	13.66 ± 0.11	5
ANC61	1396 ± 2	0.25						14.15 ± 0.32	6
ANC34	1400 ± 2	0.25	e	66 ± 9	65 ± 4				
ANC65	1398 ± 2	0.25	e	59 ± 3	64 ± 4		0.0054(2)	13.99 ± 0.18	6
ANC6	1393 ± 5	0.25	e	59	65				
ANC73	1400 ± 3	0.78	e	92	62				
			b			~150			
ANC38	1401 ± 1	1.5	b			203 ± 32	0.0061(2)	14.28 ± 0.16	6
ANC39	1400	8.25	b			324 ± 42	0.0065(2)	14.82 ± 0.08	6
ANC36	1400 ± 2	48	b			611 ± 116	0.0066(2)	15.19 ± 0.15	6
ANC9*	1402 ± 8	179	b			1024 ± 130			
ANC35	1402 ± 2	408	b			1540 ± 141	0.0069(2)	15.24 ± 0.26	6
ANC48	1397 ± 1	1102	b			2283 ± 290	0.0070(2)	15.48 ± 0.21	6
ANC42	1289 ± 8	0.017	e	39 ± 3	71 ± 5		0.0035(3)		
ANC13	1278 ± 2	0.017	e	26 ± 2	81 ± 4				
ANC46	1293 ± 6	0.017	e†	36	79		0.0038(3)	13.03 ± 0.19	6
				44 ± 3	66 ± 2				
ANC17	1284 ± 5	0.067	e†	32, 33	71, 77		0.0044(3)	13.46 ± 0.09	5
				43 ± 2	66 ± 2				
ANC14	1283 ± 11	0.25	e	45 ± 3	68 ± 3				
ANC41	1291 ± 10	0.25	e	47 ± 4	65 ± 3		0.0051(3)	13.53 ± 0.15	6
ANC15	1283 ± 11	0.67	e	46 ± 4	67 ± 5				
ANC40	1301 ± 2	1.5	e	73 ± 4	62 ± 2		0.0063(2)	14.14 ± 0.09	5
ANC18	1294	3	e	69 ± 7	63 ± 5		0.0064(2)	14.34 ± 0.12	5
ANC5	1294 ± 4	6	e	66 ± 6	68 ± 3				
ANC58	1298	8.25	e	81	62		0.0066(2)	14.77 ± 0.17	5
ANC16	1294 ± 2	24						15.07 ± 0.31	5
ANC43	1303 ± 1	48	b		189 ± 21		0.0068(2)	14.98 ± 0.20	5
ANC4	1302 ± 2	113	b		223 ± 32				
ANC30	1300 ± 2	401					0.0072(2)	15.25 ± 0.15	5
ANC45	1303 ± 1	400	b‡	30, 27	77, 80	468 ± 59	0.0072(2)	15.34 ± 0.18	6
ANC59	1299 ± 2	1077	b			673 ± 120	0.0072(2)	15.87 ± 0.19	6
ANC62	1392 ± 2	380	b			1988 ± 215	0.0073(2)	15.84 ± 0.12	5
	+1300 ± 1	1342							
ANC25	1197 ± 5	0.017	e	26 ± 2	84 ± 3		0.0021(3)	11.99 ± 0.34	8
ANC64	1193 ± 13	0.017	e	25 ± 3	83 ± 1		0.0024(5)	11.88 ± 0.18	6
ANC26	1192 ± 8	0.083	e	28 ± 1	79 ± 3		0.0037(5)	12.83 ± 0.17	6
ANC27	1200 ± 2	0.83	e	34 ± 3	71 ± 3		0.0051(5)	13.64 ± 0.29	5
ANC49	1198 ± 4	4.5	e	40 ± 2	67 ± 3		0.0056(3)	14.09 ± 0.18	7
ANC24	1200	24.8	e	54 ± 2	64 ± 3		0.0063(3)	14.65 ± 0.20	5
ANC72	1199 ± 1	192	e/b	85, 92, 59	67 ± 1				
ANC28	1201	400	b			140 ± 14	0.0072(2)	15.31 ± 0.22	6
ANC31	1200 ± 2	1063	b			169 ± 24	0.0072(2)	15.61 ± 0.11	6
ANC71	1402 ± 2	331	b			2089 ± 349	0.0076(2)	16.26 ± 0.18	6
	+1202 ± 2	2141							
ANC19	1102 ± 3	0.25	e	25, 27	86 ± 1		0.0	8.92 ± 0.23§	4
ANC66	1100 ± 1	0.33	e	26 ± 2	86 ± 3		0.0009(3)	10.62 ± 0.28§	7
ANC63	1199 ± 3	0.67	e	26 ± 2	83 ± 2		0.0029(3)	12.66 ± 0.13	5
ANC48′	1100 ± 1	0.67					0.0031(5)	12.34 ± 0.18	7
ANC20	1103 ± 2	2					0.0042(3)	13.17 ± 0.12	5
ANC53	1099 ± 2	2	e	30 ± 1	76 ± 3		0.0045(5)	13.25 ± 0.29	6
ANC21	1104 ± 1	8.25					0.0044(3)	13.43 ± 0.15	4
ANC54	1100	8.25	e	31 ± 2	76 ± 3		0.0055(3)	13.66 ± 0.19	6
ANC50	1100 ± 1	30.3	e	35 ± 1	67 ± 2		0.0058(3)	14.22 ± 0.21	5
ANC52	1100 ± 1	30					0.0062(3)	14.18 ± 0.24	4
ANC55	1100 ± 1	95	e	41 ± 5	66 ± 4		0.0062(3)	14.47 ± 0.10	5
ANC22	1104 ± 2	96					0.0064(3)	14.35 ± 0.19	6
ANC23	1105 ± 2	412	e	49 ± 5	68 ± 2		0.0068(3)	14.60 ± 0.22	7
ANC29	1098 ± 1	1105	e	59, 59	66, 59		0.0071(3)	14.99 ± 0.21	7

Note: Starting material = glass of anorthite composition. Temperature range quoted represents range of temperatures measured during course of annealing. Quoted annealing times exclude initial ~1.25–1.5 minutes (0.021–0.025 h) after loading sample into furnace; during this time the sample temperature rose rapidly to within ~10–20 °C of the furnace temperature (1100, 1200, 1300, or 1400 °C).

* 1.4 g of sample, rather than 0.4, 0.45, or 0.5 g was used for these experiments.

** 1 standard deviation quoted only for three or more separate measurements.

† Spacings and orientations of e reflections from different grains formed two populations.

‡ Diffraction patterns from two regions of this sample gave diffuse e reflections.

§ Sample contained relict glass.

perpendicular to ϵ_2 and is quite close to the (001) plane; it rotates to some extent with increasing Al-Si order (Fig. 3).

Finally, scalar strains have been calculated from the principal strains, following Redfern and Salje (1987), as

$$\epsilon_s = \sqrt{\sum_{i=1-3} \epsilon_i^2}. \quad (1)$$

These are given in Table 1 with standard deviations propagated from the standard deviations of the lattice parameter data. (Note that this error propagation does not include uncertainties in the fixed reference state.) Values of ϵ_s are between zero and ~0.008 and increase smoothly with increasing annealing time at a given temperature (Fig. 4).

The $C\bar{1} \rightleftharpoons I\bar{1}$ transition is associated with a special point on the Brillouin zone boundary, and the relationship between the spontaneous strain and the order parameter is expected to be $\epsilon_s \propto Q_{od}^2$. This relationship has been verified for anorthite by Carpenter et al. (1990c) who used estimated site occupancies from structure refinements to determine absolute values of Q_{od} in crystals with different degrees of Al-Si order. The calibration seems to work in spite of the fact that spontaneous strains are determined, more conventionally, from lattice parameter measurements made in situ at high temperatures. Distortions that result from the $C2/m \rightleftharpoons C\bar{1}$ or $I\bar{1} \rightleftharpoons P\bar{1}$ transitions appear to be successfully filtered out (see discussion in Carpenter et al., 1990c). It should be emphasized that the resulting values of Q_{od} represent averages over a macroscopic length scale. In the present case, the synthetic anorthite crystals do not have homogeneous degrees of order on a local (unit cell) length scale. The structures are known to be modulated in the early stages of ordering, and the diffuseness of superlattice reflections also suggests local heterogeneities. Figure 4 thus implies that the square of the average degree of order varies approximately linearly with ln t over a limited interval. Carpenter (1988) sugested, on the basis of some preliminary data, that $\epsilon_s^2 \propto \ln t$ provides a reasonable description of the ordering, but this may be an artifact of the requirement that Q_{od} must level off to its equilibrium value at long annealing times.

The Al-Si ordering is accompanied by a small but measurable volume reduction. Redfern (1989) has shown that any volume change accompanying the $I\bar{1} \rightleftharpoons P\bar{1}$ transition is negligibly small. Volume changes observed here may therefore be ascribed entirely to the $C\bar{1} \rightleftharpoons I\bar{1}$ transition. To a first approximation the excess volume, V, due to ordering might be expected to vary with Q_{od}^2 (Carpenter, 1991b); ϵ_s, which is proportional to Q_{od}^2, is indeed a reasonably linear function of unit-cell volume, though there is considerable scatter (Fig. 5). A least-squares fit to the data shown in Figure 5 and the calibration of Q_{od} in terms of ϵ_s from Carpenter et al. (1990c) give a unit-cell volume change of -5.4 Å^3 for Q_{od} changing from 0 to 1. Hence, a_v would be -0.039 cal/bar/mol in a relationship of the form $V = \frac{1}{2}(a_v Q_{od}^2)$. Note that V is the excess volume resulting from the $C\bar{1} \rightleftharpoons I\bar{1}$ transition and that a_v is negative because the volume decreases with increasing Q_{od}.

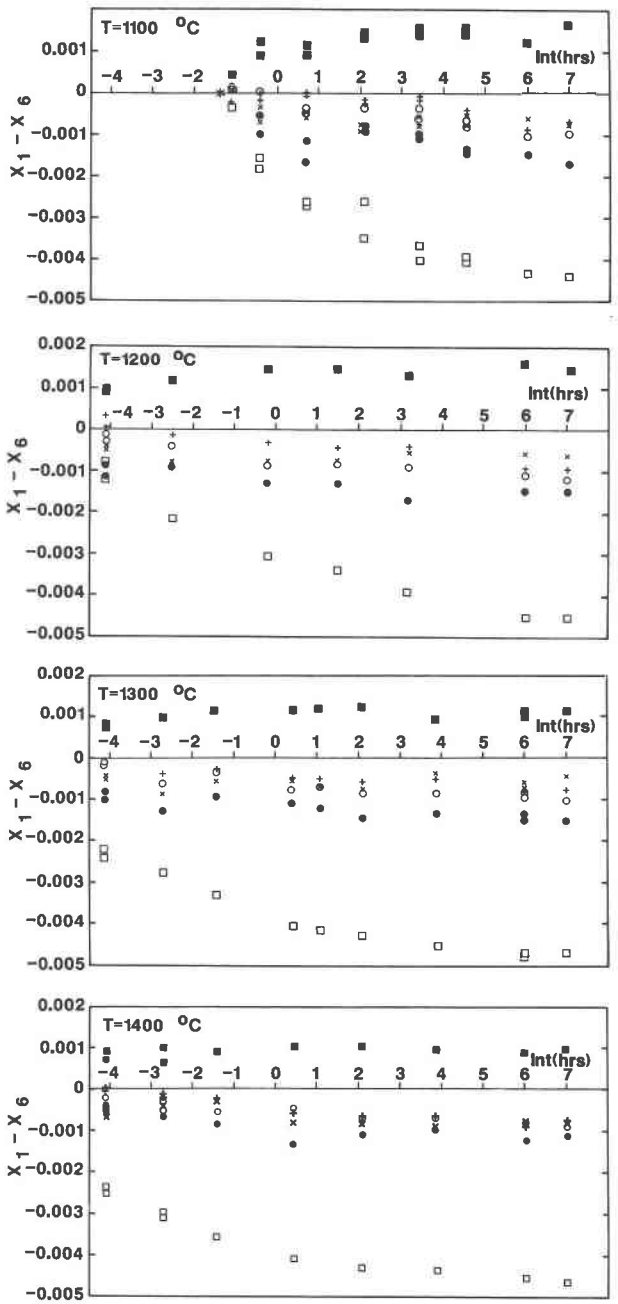

Fig. 1. Variation of individual components, x_1–x_6, of the strain tensor for the $C\bar{1} \rightleftharpoons I\bar{1}$ transition in synthetic anorthite crystals as a function of annealing time (x_1 = filled circles, x_2 = ×, x_3 = +, x_4 = filled squares, x_5 = open circles, x_6 = open squares).

Enthalpy variations

Heat of solution values for the synthetic anorthite samples fall between 8.92 ± 0.23 and 16.26 ± 0.18 kcal/mol (Table 1). As discussed below, most of the ~7 kcal/mol

TABLE 2. Lattice parameters for synthetic anorthites described in Table 1

Sample no.	a (Å)	b (Å)	c (Å)	α (°)	β (°)	γ (°)	V (Å³)
ANC32	8.183(1)	12.877(2)	14.180(3)	93.32(2)	115.71(1)	90.98(1)	1342.6(5)
ANC60	8.184(1)	12.874(2)	14.184(3)	93.33(1)	115.73(1)	91.00(1)	1342.6(5)
ANC11	8.182(1)	12.878(2)	14.178(3)	93.28(2)	115.71(1)	91.05(2)	1342.2(6)
ANC33	8.182(1)	12.880(1)	14.180(2)	93.31(1)	115.73(1)	91.07(1)	1342.2(5)
ANC65	8.181(1)	12.879(1)	14.179(2)	93.26(1)	115.73(1)	91.12(1)	1341.9(5)
ANC38	8.177(1)	12.872(1)	14.172(2)	93.22(1)	115.72(1)	91.18(1)	1340.1(4)
ANC39	8.179(1)	12.872(1)	14.174(2)	93.21(1)	115.74(1)	91.20(1)	1340.3(4)
ANC36	8.180(1)	12.871(1)	14.174(2)	93.21(1)	115.75(1)	91.21(1)	1340.3(3)
ANC35	8.178(1)	12.872(1)	14.173(2)	93.22(1)	115.75(1)	91.23(1)	1339.9(3)
ANC48	8.179(1)	12.872(1)	14.175(2)	93.20(1)	115.76(1)	91.24(1)	1340.2(3)
ANC42	8.179(2)	12.877(2)	14.178(4)	93.34(2)	115.69(2)	90.96(2)	1341.9(8)
ANC46	8.181(2)	12.876(2)	14.179(3)	93.33(2)	115.70(1)	90.99(2)	1342.1(7)
ANC17	8.177(1)	12.872(2)	14.177(3)	93.29(2)	115.74(1)	91.03(2)	1340.5(6)
ANC41	8.180(2)	12.876(2)	14.176(3)	93.25(2)	115.71(1)	91.09(2)	1341.5(6)
ANC40	8.179(1)	12.876(2)	14.177(2)	93.21(1)	115.74(1)	91.18(1)	1341.5(5)
ANC18	8.178(1)	12.874(2)	14.176(2)	93.20(1)	115.74(1)	91.19(1)	1340.5(5)
ANC58	8.176(1)	12.873(2)	14.176(3)	93.19(1)	115.75(1)	91.20(1)	1340.1(5)
ANC43	8.177(1)	12.878(2)	14.177(3)	93.21(1)	115.75(1)	91.23(1)	1340.8(5)
ANC30	8.177(1)	12.875(1)	14.174(2)	93.19(1)	115.75(1)	91.26(1)	1340.1(4)
ANC45	8.176(1)	12.873(1)	14.172(1)	93.18(1)	115.74(1)	91.25(1)	1339.7(3)
ANC59	8.176(1)	12.877(1)	14.175(2)	93.18(1)	115.77(1)	91.25(1)	1340.1(4)
ANC62	8.177(1)	12.875(1)	14.174(2)	93.17(1)	115.77(1)	91.26(1)	1340.1(4)
ANC25	8.178(2)	12.877(2)	14.181(3)	93.40(1)	115.70(1)	90.80(2)	1342.0(7)
ANC64	8.180(2)	12.878(3)	14.182(4)	93.37(3)	115.69(2)	90.85(3)	1342.7(8)
ANC26	8.180(2)	12.873(2)	14.179(4)	93.30(2)	115.71(1)	90.96(3)	1341.4(7)
ANC27	8.177(2)	12.874(2)	14.180(4)	93.23(2)	115.76(2)	91.06(3)	1340.6(9)
ANC49	8.177(2)	12.873(2)	14.177(4)	93.21(2)	115.75(2)	91.10(2)	1340.5(8)
ANC24	8.174(2)	12.876(2)	14.178(3)	93.20(2)	115.75(1)	91.16(2)	1340.2(7)
ANC28	8.176(1)	12.876(1)	14.174(2)	93.14(1)	115.78(1)	91.23(1)	1339.9(5)
ANC31	8.176(1)	12.875(1)	14.175(2)	93.15(1)	115.78(1)	91.23(1)	1339.9(4)
ANC71	8.176(1)	12.878(1)	14.177(2)	93.14(1)	115.81(1)	91.26(1)	1339.9(5)
ANC19	8.187(2)	12.883(3)	14.182(4)	93.53(2)	115.70(2)	90.71(2)	1344.0(8)
ANC66	8.188(2)	12.884(3)	14.177(4)	93.47(2)	115.70(1)	90.75(2)	1343.9(7)
ANC63	8.183(1)	12.879(2)	14.177(3)	93.33(2)	115.70(1)	90.89(2)	1342.8(6)
ANC48′	8.179(2)	12.874(2)	14.174(4)	93.35(2)	115.68(1)	90.92(3)	1341.4(7)
ANC20	8.178(1)	12.875(2)	14.180(3)	93.31(2)	115.72(1)	91.01(2)	1341.3(6)
ANC53	8.174(2)	12.877(2)	14.179(4)	93.28(2)	115.69(2)	91.02(3)	1341.3(9)
ANC21	8.181(1)	12.873(2)	14.177(3)	93.25(2)	115.71(1)	91.01(2)	1341.5(6)
ANC54	8.180(2)	12.871(2)	14.176(3)	93.22(2)	115.71(1)	91.11(2)	1340.9(7)
ANC50	8.178(2)	12.873(2)	14.176(3)	93.19(2)	115.70(1)	91.13(2)	1341.2(6)
ANC52	8.177(1)	12.876(2)	14.179(3)	93.19(2)	115.72(1)	91.17(2)	1341.2(6)
ANC55	8.177(1)	12.876(2)	14.178(3)	93.19(2)	115.75(1)	91.16(2)	1340.7(5)
ANC22	8.176(2)	12.873(2)	14.174(4)	93.17(2)	115.74(1)	91.17(2)	1340.1(7)
ANC23	8.176(2)	12.875(2)	14.174(3)	93.19(2)	115.76(1)	91.21(2)	1339.9(6)
ANC29	8.174(2)	12.873(2)	14.174(4)	93.14(2)	115.76(1)	91.22(2)	1339.6(7)

Note: Numbers in brackets indicate 1 σ expressed as the uncertainty in the last significant figure.

variation is ascribed to the effects of Al-Si ordering. Absolute heats of solution are notoriously sensitive to other factors, however, and three additional contributions must be considered. First, enthalpies of fusion for silicates tend to be large relative to enthalpies of ordering, and the presence of a small amount of glass mixed in with crystals can have a marked effect on ΔH_{soln} for a given sample. Two samples contained relict glass that could easily be distinguished optically (ANC19, 15 min at 1100 °C; ANC66, 20 min at 1100 °C), and their ΔH_{soln} values are clearly lower than would be expected (ANC66 is plotted in Fig. 6, but ANC19 is not). Glass was not observed in any of the other samples by optical or electron microscopy, and given the rapid crystallization rates of anorthite glass at 1200 °C, 1300 °C, and 1400 °C, this problem is unlikely to be significant. Second, the synthetic anorthite samples contained a fine dispersion of an additional unidentified phase (described in Carpenter, 1991a). The small inclusions appeared to be present at about the same volume fraction ($\ll 1\%$) in all the samples so that, although they may have affected the absolute values of ΔH_{soln}, they probably did not contribute to the observed enthalpy differences between samples. Third, all the anorthite crystals contained abundant albite twinning. Twins are defects that must contribute some excess enthalpy. The scale of twinning did not appear to change with annealing time at a constant temperature, but crystals prepared at 1400 °C had slightly coarser twins on average than those prepared at 1100 °C. It is possible that some of the enthalpy differences between anorthite samples prepared at different temperatures are due to changes in the twin size distribution, although no positive evidence for this has been found. A plot of ϵ_s, which should not be sensitive to twinning variations, against ΔH_{soln} (Fig. 6) does not reveal systematic differences between samples as a function of annealing temperature.

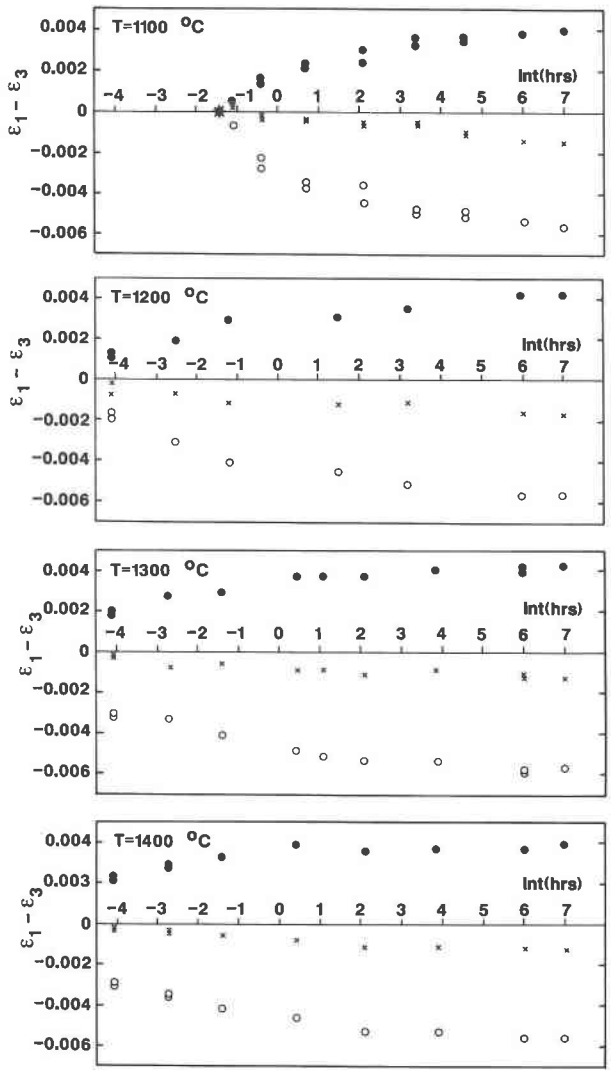

Fig. 2. Variation with annealing time of the principal strains, ϵ_1, ϵ_2, ϵ_3, derived from the strain components given in Figure 1. Note that $\epsilon_2 \approx 0$ and $\epsilon_1 \approx -\epsilon_3$, implying that the net strain is almost a pure shear (ϵ_1 = filled circles, ϵ_2 = crosses, ϵ_3 = open circles).

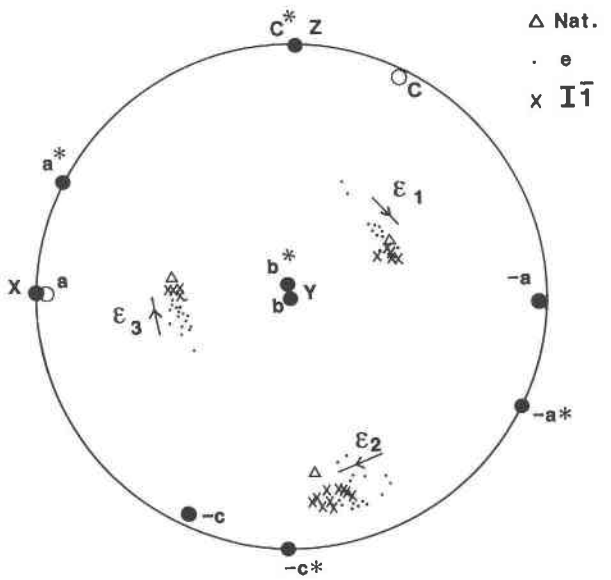

Fig. 3. Stereographic projection showing the orientation of the principal strain axes, ϵ_1, ϵ_2, ϵ_3, with respect to the real (**a**, **b**, **c**) and reciprocal (**a***, **b***, **c***) lattice vectors of anorthite. *X*, *Y*, and *Z* represent the coordinate system used to calculate the strains (see Redfern and Salje, 1987). Arrows indicate the change in orientation of the principal strains with increasing Al-Si order. Data for the natural sample (Nat.) refer to Val Pasmeda anorthite (lattice parameter data from Carpenter et al., 1985).

The two most significant results of the calorimetric study are illustrated in Figures 6 and 7. Figure 6 shows an approximately linear relationship between ϵ_s and ΔH_{soln} for all the synthetic anorthites, with the exception of the most ordered samples, which show increasing ΔH_{soln} at approximately constant ϵ_s, and the two samples containing glass. The implication is that Q^2_{od} varies approximately linearly with the excess enthalpy of ordering, *H*, independently of heat treatment. Extrapolation of the straight line to $\epsilon_s = 0$ and the calibration of ϵ_s in terms of Q_{od} from Carpenter et al. (1990c) allow the relationship between *H* and Q_{od} to be analyzed quantitatively. Figure 7 shows that, over a long time interval, ΔH_{soln} for the synthetic anorthite samples is linear with ln *t*. This in turn, following from the relationship in Figure 6, demonstrates that the ordering follows an empirical rate law of the form $Q^2_{od} \propto \ln t$ to a reasonable approximation.

The implications of these relationships for the energetics of individual Al-Si exchanges, the defect energies of antiphase boundaries (APBs), and the overall kinetic behavior are set out in the following sections.

Al-Si exchange energies

In discussing the origin of enthalpy variations associated with Al-Si ordering it is convenient, though some-

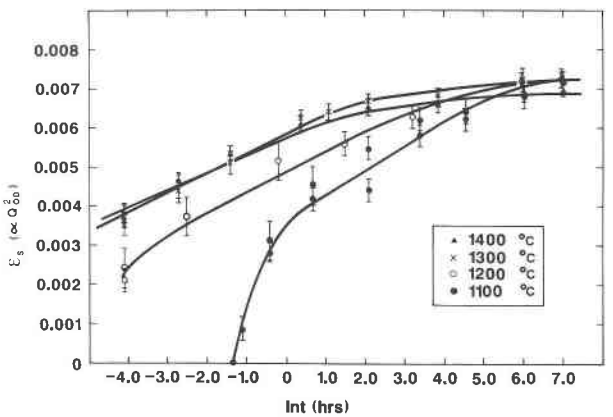

Fig. 4. Variation of the scalar strain, ϵ_s, with the logarithm of annealing time, *t*. Approximately linear segments of ϵ_s occur over limited ranges of ln *t*.

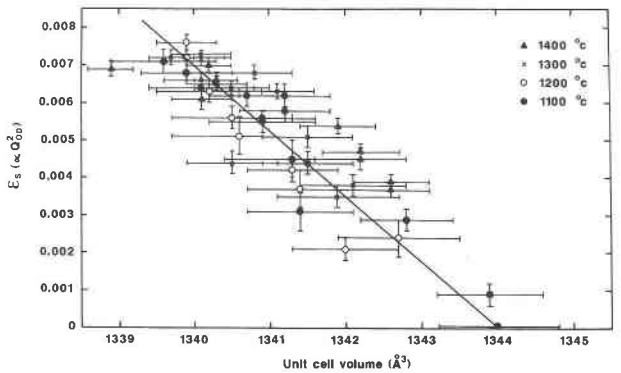

Fig. 5. Approximate linear relationship between the scalar spontaneous strain, ϵ_s ($\propto Q_{od}^2$), and unit-cell volume, showing that the excess volume due to $C\bar{1} \rightarrow I\bar{1}$ ordering can be described as proportional to Q_{od}^2.

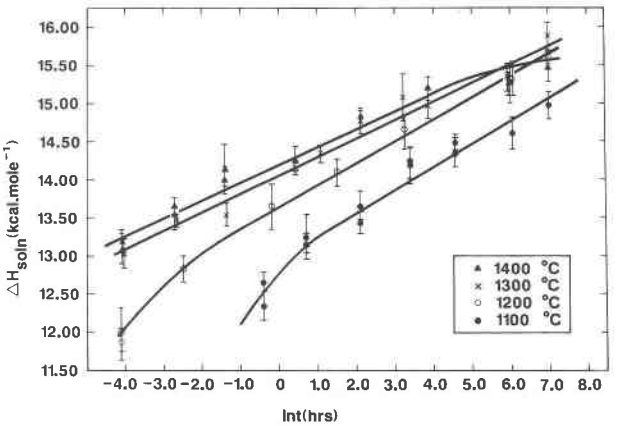

Fig. 7. Variation of heat of solution, ΔH_{soln}, with the natural logarithm of annealing time, t, for crystals of synthetic anorthite prepared from glass. Linear trends are apparent for a restricted range of ln t.

what arbitrary, to distinguish between thermal energies arising from vibrational effects, elastic energies associated with macroscopic distortions of a crystal, and chemical bond energies assigned to the energies of individual -Al-O-Al-, -Si-O-Si-, and -Al-O-Si- linkages (Carpenter, 1988). The vibrational contributions are expected to be relatively small, and since for anorthite the strains are also small, the elastic energy, $\frac{1}{2} \Sigma_{i,k} C_{ik} x_i x_k$, will be negligible. Here x_i and x_k are components of the spontaneous strain and C_{ik} represents the elastic constants, with $i, k = 1$–6. The entire enthalpy change can therefore be discussed in terms of local changes in bonding described by the reaction

$$\text{(-Si-O-Si-)} + \text{(-Al-O-Al-)} \rightarrow 2\text{(-Al-O-Si-)}. \quad (2)$$

This reaction can be calibrated in exactly the same manner as for Al-Si ordering in cordierite (Putnis and Angel, 1985; Putnis et al., 1985, 1987; Salje, 1987; Putnis, 1988). First, however, the number of Al-O-Al linkages may be defined in terms of the macroscopic order parameter, Q_{od}, as follows (after Becker, 1978).

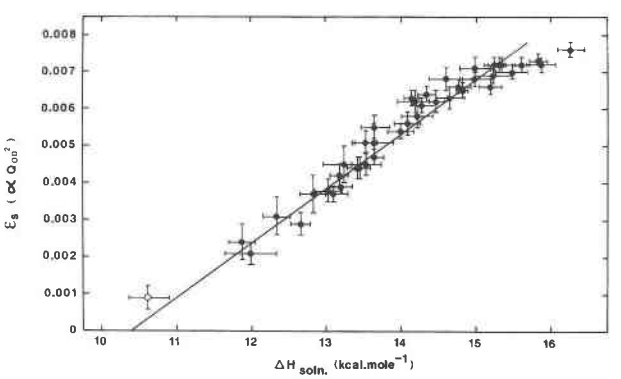

Fig. 6. Scalar strain, ϵ_s, plotted as a function of heat of solution, ΔH_{soln}, for synthetic anorthite crystals prepared from glass. The straight line has been drawn by eye, excluding data for ANC19 (not shown) and ANC66 (open circle, $\epsilon_s \sim 0.001$) since these two samples contained some relict glass. Separate trends for samples prepared at different temperatures have not been discerned.

For a crystal consisting of only A and B atoms in equal proportions, let the probability of finding B next to A be q. The number of A-B linkages, n_{AB}, is then given by

$$n_{AB} = \tfrac{1}{2} N z q \quad (3)$$

where N is the total number of atoms and z is their coordination number. For a fully ordered arrangement of atoms, with the A and B atoms alternating on sublattice sites designated α and β, q will be 1. For a random distribution of A and B atoms on the α and β sites, q will be ½. A short-range order parameter, σ, may be defined such that it takes values between 0 for complete disorder and 1 for complete order as

$$\sigma = 2q - 1 \quad (4)$$

or

$$q = \frac{\sigma + 1}{2}. \quad (5)$$

The number of A-B linkages in terms of σ is then

$$n_{AB} = \tfrac{1}{4} N z (\sigma + 1). \quad (6)$$

Now, if the probability of finding an A atom on an α site (or B on a β site) is p, a long-range order parameter, Q, may be defined as

$$Q = 2p - 1 \quad (7)$$

or

$$p = \frac{Q + 1}{2}. \quad (8)$$

Since $p = 1$ for complete order and $p = \frac{1}{2}$ for a random distribution, Q varies between 1 and 0. The number of

A-B bonds with A on α sites is $\frac{1}{2}Nzp^2$, and the number of A-B bonds with A on β sites is $\frac{1}{2}Nz(1 - p)^2$. Hence

$$n_{AB} = \tfrac{1}{2}Nzp^2 + \tfrac{1}{2}Nz(1 - p)^2. \quad (9)$$

Substituting for p in terms of Q yields

$$n_{AB} = \tfrac{1}{4}Nz(Q^2 + 1). \quad (10)$$

Comparison of Equation 10 with Equation 6 shows that the relationship between the short-range order parameter σ, which is effectively a bond counting operator, and the long-range order parameter, Q, is

$$\sigma = Q^2. \quad (11)$$

This strictly applies only when the degree of order is homogeneous throughout the crystal of interest. If the degree of order varies on a local scale, the mean value of σ, $\langle\sigma\rangle$, only approximates to Q_{od}^2.

In the present instance, it is more informative to define σ in terms of the number of A-A linkages, n_{AA}. The probability, m, of finding A next to A will vary between 0 and $\frac{1}{4}$ and may be expressed in terms of q as

$$m = \tfrac{1}{2}(1 - q) \quad (12)$$

or

$$q = 1 - 2m. \quad (13)$$

Substituting m for q in the definition of σ (Eq. 4) gives

$$\sigma = 1 - 4m \quad (14)$$

and, since

$$n_{AA} = \tfrac{1}{2}Nzm \quad (15)$$

it follows that

$$\sigma = 1 - \frac{8n_{AA}}{Nz}. \quad (16)$$

Finally, defining $N_{Al\text{-}Al}$ as the number of Al-O-Al linkages per formula unit of anorthite ($CaAl_2Si_2O_8$) gives

$$\sigma = 1 - \frac{N_{Al\text{-}Al}}{2} \quad (17)$$

$$\rightarrow \quad N_{Al\text{-}Al} = 2(1 - \sigma) \quad (18)$$

$$\rightarrow \quad N_{Al\text{-}Al} = 2(1 - Q_{od}^2) \quad (19)$$

since $N = 4$ per formula unit and $z = 4$ (each tetrahedron is coordinated to four other tetrahedra).

From these geometrical arguments, it follows that Q_{od}^2 for the synthetic anorthite crystals should be linearly dependent on the average number of Al-O-Al linkages present. The linear relationship between Q_{od}^2 and the excess enthalpy of ordering, H, implied by Figure 6 thus suggests that H is proportional to $N_{Al\text{-}Al}$ to a reasonable approximation. In other words, the enthalpy change, Δh, resulting from exchanging individual Al and Si atoms according to the reaction specified in Equation 2, is constant and does not vary with the degree of order. Two moles of such exchanges are required to produce 1 mol of fully ordered anorthite ($CaAl_2Si_2O_8$) from 1 mol of disordered anorthite. Taking a slope of 0.0015 ± 0.0003 units of strain per kcal of ΔH_{soln} from Figure 6 and the calibration

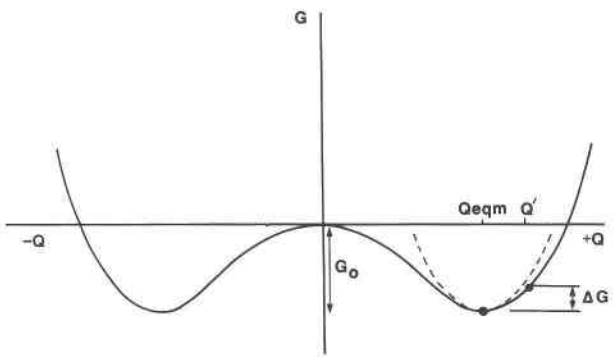

Fig. 8. Schematic variation of excess free energy, G, as a function of the order parameter, Q, at some temperature below T_c for a second-order phase transition. G_0 indicates the excess energy for a crystal with equilibrium order, Q_{eqm}. The dashed line represents a harmonic approximation [$\Delta G \propto (\Delta Q)^2$] for the excess energy, ΔG, of a crystal as a function of its deviation from equilibrium, $\Delta Q = Q' - Q_{eqm}$.

$Q_{od} = 10.1\ (\pm\ 0.5)\sqrt{\epsilon_s}$ (Carpenter et al., 1990c) gives $H = -6.5 \pm \sim 2$ kcal/mol for Q_{od} going from zero to one. This gives $\Delta h = -3.3 \pm \sim 1$ kcal per mole of Al-Si exchanges, which may be compared with ~ -8.1 and ~ -6.0 kcal estimated for the equivalent exchange reaction in cordierite and albite by Putnis and Angel (1985). Most of the synthetic anorthite samples are not homogeneous with respect to their degree of Al-Si order on a local unit-cell scale, however, and are more ordered locally than the average order parameter suggests. The mean values of $N_{Al\text{-}Al}$ determined from Q_{od} are therefore overestimated, and this value of Δh should be treated as only a minimum enthalpy for the Al-Si exchange reaction.

If the total enthalpy of ordering in anorthite is ~ -7 kcal/mol and H varies linearly with Q_{od}^2, the value of H for Val Pasmeda anorthite ($Q_{od} = 0.92$, from Carpenter et al., 1990c) would be ~ -5.9 kcal/mol. This is larger than the value of ~ -3.7 kcal/mol estimated by Carpenter et al. (1985), perhaps because the most disordered crystals used in the present study had less short-range order than would be present in the extrapolated $C\bar{1}$ structural state used by Carpenter et al. (1985) to represent $Q_{od} = 0$.

Defect energies of APBs

Antiphase boundaries are usually regarded as defects in otherwise well-ordered crystals. As such, they have an associated excess energy and, given sufficient time, will anneal out in the manner described by Carpenter (1991a). They separate domains with degrees of order represented by +Q and −Q but, rather than being completely steplike in character, have a finite width and some continuous gradient in Q. The excess energy can be modeled by referring to the energetics of ordering, as discussed for example by Allen and Cahn (1979) and as illustrated in Figure 8. There are two main contributions to consider. Since the APBs have a finite volume and are less well

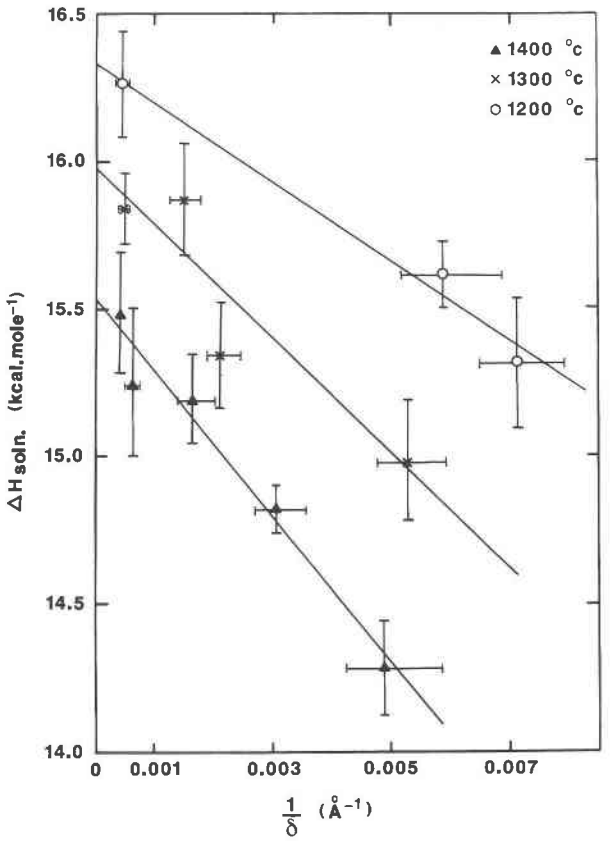

Fig. 9. Variation of heat of solution with the inverse of APD size, δ, for synthetic anorthite crystals with type b APDs. The straight lines represent least-squares fits to the data and have slopes of −246, −190, and −136 kcal/mol/Å for crystals annealed at 1400, 1300, and 1200 °C, respectively. Note that ΔH_{soln} is endothermic and hence that increasing ΔH_{soln} corresponds to decreasing enthalpy of the crystals.

ordered than the bulk of the crystals, there will be a volume term related to the energy of ordering, G_0 in Figure 8. The value of Q must be zero at some point within the APB, and gradients to $+Q$ and $-Q$ on either side will contribute a gradient energy. Both terms will usually be positive (energetically unfavorable), and whereas the gradients may or may not steepen with increasing Q, the volume term will become larger (more positive) as temperature decreases because G_0 increases in magnitude. The normal expectation is that the excess energy relative to a homogeneous ordered crystal will increase with falling temperature in some way that depends in detail on the variation of G_0.

The first hint that the calorimetric data might have sufficient resolution to show enthalpy variations because of the APBs alone is provided by the increase in ΔH_{soln} at almost constant strain for crystals with high degrees of order (Fig. 6). Once a certain domain size is reached, the value of ϵ_s from X-ray powder diffraction measurements gives a measure of Q_{od}^2 for the homogeneous domains. Some Al-O-Al linkages will still be present at the APBs, however, and the proportion of these will diminish, releasing energy, as the domains coarsen even if Q_{od} within the domains remains constant. If the APBs are treated as surfaces or thin films between domains that have a mean diameter of δ, the total APB area will vary with δ^2. The total APD volume will vary with δ^3 so that the APB "surface" area per unit volume will vary with $1/\delta$. Figure 9 indicates that ΔH_{soln} for crystals with different type b APD sizes is a linear function of $1/\delta$. In other words, the enthalpy of the crystals varies linearly with the APB surface area, as would be expected if the domains coarsened at constant Q_{od}. This allows the enthalpy per unit area of APB to be calculated for anorthite crystals at 1200, 1300, and 1400 °C once an absolute measure of the surface area per unit volume, S_v, has been determined.

Smith and Guttman (1953) have shown that S_v for three dimensional textures of this kind is related directly to δ by $S_v = 2/\delta$, and Nord and Lawson (1989) have made use of this relationship to follow surface area variations of twin domains in crystals of the ilmenite-hematite solid solution. The measured values of δ in ångstroms, given in Table 1, can therefore be converted into values of S_v, in cm^2 per mole of $CaAl_2Si_2O_8$, quite simply as

$$S_v = \frac{2.018 \times 10^{10}}{\delta} \qquad (20)$$

using a molar volume of 100.9 cm^3 for anorthite. The slopes of the straight lines in Figure 9 (−246, −190, and −136 kcal/mol/Å) thus give $1.22 \pm \sim 0.30 \times 10^{-5}$, $0.94 \pm \sim 0.20 \times 10^{-5}$, and $0.67 \pm \sim 0.20 \times 10^{-5}$ cal·cm^{-2} as the excess enthalpy resulting from the presence of APBs in the crystals annealed at 1400, 1300, and 1200 °C, respectively. The effect of introducing APBs with $\delta = 500$ Å into crystals equilibrated at these three temperatures would be to increase their enthalpies by ~490 cal/mol (1400 °C), ~380 cal/mol (1300 °C), and ~270 cal/mol (1200 °C), for example. No information about the accompanying excess entropy can at present be offered, however.

A surprising result is that, contrary to expectation, the excess enthalpy of the APBs appears to decrease with falling temperature. Figure 10 shows that the APBs might actually become stable at some lower temperature. A linear extrapolation that ignores the experimental uncertainties shows the excess enthalpy becoming negative at ~950 °C (Fig. 10). If this is correct, it implies that the local structure of the APBs cannot be represented simply by a gradient in Q_{od} for Al-Si ordering on an $I\bar{1}$ basis, $Q_{od}^{I\bar{1}}$. One obvious possibility is that some ordering on the basis of the local $C\bar{1}$ symmetry occurs and that this couples with the gradients in $Q_{od}^{I\bar{1}}$ in much the same way as has been suggested for the incommensurate plagioclase structure (see Carpenter, 1991a and references therein). The observed APB energies might then be used to estimate the energy contribution of the periodic APBs in intermediate plagioclase crystals. For crystals of composition An_{70}, the spacing between the periodic APBs of the

IC structure is ~45 Å (Smith and Brown, 1988). Treating the APBs as uniformly parallel and straight features then gives a total surface area of 2.24×10^8 cm²/mol. From Figure 10, the APB enthalpy at ~700 °C would be $\sim -0.7 \times 10^{-5}$ cal/mol, and hence, the total enthalpy of the APBs relative to homogeneous crystals with $I\bar{1}$ order would be ~−1.6 kcal/mol. The equivalent difference in the enthalpy of ordering between $I\bar{1}$ and IC structures at about the same composition falls between ~−0.7 and ~−1.9 kcal/mol from calorimetric measurements on natural samples (Carpenter et al., 1985). Given the crudity of the model and the fact that experimental uncertainties have been ignored, the close agreement between these numbers must be regarded as fortuitous, but the calculation at least provides permissive evidence that the two types of APBs in IC and $I\bar{1}$ structures might be related in this way.

It is not clear from published models of APD coarsening that local ordering at APBs, as opposed to impurity segregation, would modify the $\delta^2 \propto t$ rate law. According to Allen and Cahn (1979), the change in APB energy should not by itself be significant in this respect. If the free energy of the APBs becomes negative, however, quite different behavior will obviously result because there would be no energy dissipation associated with coarsening.

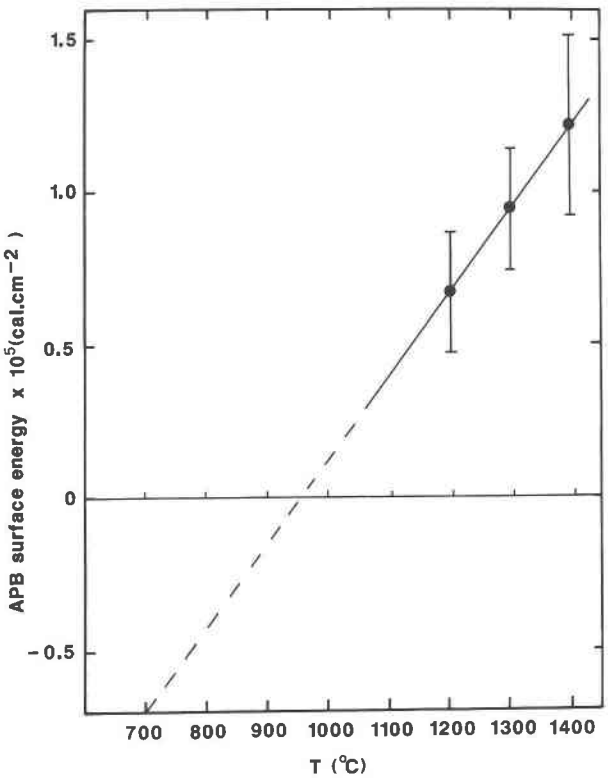

Fig. 10. Excess energies of APBs, relative to homogeneous ordered crystal, expressed in terms of an enthalpy per unit area, for type b APBs. The extrapolation is designed only to illustrate that these enthalpies apparently decrease with decreasing annealing temperature and might become negative at some low temperature. Positive values imply that the APBs are defects in otherwise well-ordered crystals, whereas negative values would imply that they might become stable features.

Empirical rate equation

The experimental observations shown in Figures 4 and 7 are consistent with a rate law of the form $Q_{od}^2 \propto \ln t$ over a range of Q_{od} between ~0.6 and ~0.85. In their analysis of time-dependent order parameter behavior, Salje (1988) and Carpenter and Salje (1989) showed that this type of rate law can be anticipated for systems in which the order parameter does not remain homogenous. Even though thermodynamic data are insufficient to allow a numerical solution based on integration of the GL equation, an empirical approach using the observed logarithmic time dependence gives an internally consistent description of the kinetics, as set out here. Because of their greater linear ln t range relative to the spontaneous strain data, the enthalpy data are used for the analysis. Possible physical explanations of the overall behavior are discussed in the following section.

The simplest form of the appropriate rate law derived by Salje (1988) is

$$\langle \sigma \rangle \propto RT \ln t \tag{22}$$

which, using the definition of σ in terms Q_{od} given in Equation 11, may be rewritten as

$$Q_{od}^2 \propto RT \ln t. \tag{23}$$

The slopes of Q_{od}^2 against ln t are expected to be linear in T, and Figure 11 shows that, within the experimental uncertainties, this is indeed the case. Extrapolation to zero slope in Figure 11 gives a temperature of ~2220 °C, at which the rate of ordering would become zero. Allowing for the obvious uncertainty in the long extrapolation, this is within error of T_c for the $C\bar{1} \rightleftharpoons I\bar{1}$ transition (2010 ± 80 °C, Carpenter et al., 1990c) and is consistent with the fact that the driving force for ordering goes to zero as T_c is approached. The explicit temperature dependence given in Equation 23, RT, can be replaced by R$(T - T_c)$.

A free energy of activation, ΔG^*, is introduced by scaling the time, t, by the average time, τ, required for individual atomic exchanges, such that

$$\tau = \tau_0 \exp(\Delta G^*/RT) \tag{24}$$

where $\Delta G^* = \Delta H^* - T\Delta S^*$ and τ_0 is a constant. Equation 23 then becomes

$$Q_{od}^2 = A\mathrm{R}(T - T_c)\ln \frac{t}{\tau}. \tag{25}$$

Substituting for τ and rearranging terms gives

$$\frac{Q_{od}^2}{A\mathrm{R}(T - T_c)} = \ln t - \frac{\Delta H^*}{RT} + \frac{\Delta S^*}{\mathrm{R}} - \ln \tau_0. \tag{26}$$

Finally, to determine values for the terms in this rate equation, it is necessary to express measured variations in ΔH_{soln} as variations in Q_{od}. This is achieved by using

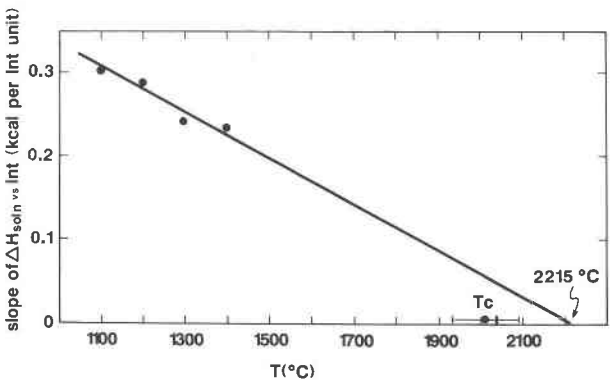

Fig. 11. Slope of ΔH_{soln} against ln t from Figure 7 plotted as a function of annealing temperature for synthetic anorthite crystals. A large slope indicates a rapid rate of ordering. The extrapolation to zero slope at 2215 °C corresponds to the driving force for ordering going to zero as T_c (= 2010 ± 80 °C) is approached.

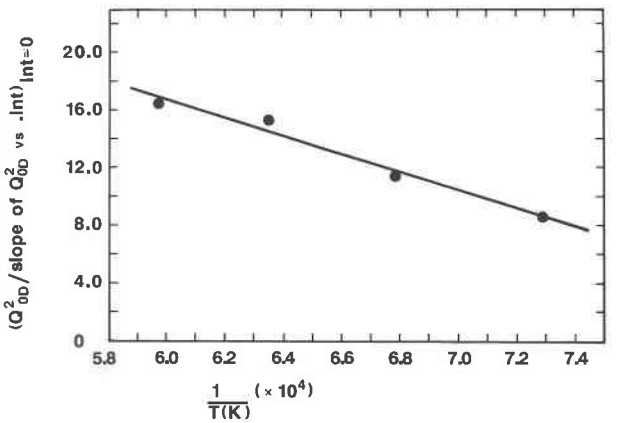

Fig. 12. Arrhenius plot of the empirical rate data given on the right hand sides of Equations 30–33 at ln t = 0. The slope gives an enthalpy of activation of 124 ± ~15 kcal/mol, and the intercept (at $1/T = 0$) gives a value for $\Delta S^*/R - \ln \tau_0$ of 54.3.

the straight line in Figure 6 for ϵ_s against ΔH_{soln} (in kcal/mol) to give

$$\epsilon_s = 0.001477(\Delta H_{soln}) - 0.01535 \quad (27)$$

and by using the relationship between ϵ_s and Q_{od} given by Carpenter et al. (1990c):

$$Q_{od} = 10.1 \sqrt{\epsilon_s}. \quad (28)$$

Thus,

$$Q^2_{od} = 0.1507(\Delta H_{soln}) - 1.566. \quad (29)$$

Using values for the slopes in Figure 7 of 0.233, 0.241, 0.288, and 0.302 kcal per ln t unit and values for ΔH_{soln} at ln t = 0 of 14.19, 14.06, 13.63, and 12.97 kcal/mol, at 1400, 1300, 1200, and 1100 °C, the enthalpy data then give

$$\frac{Q^2_{od}}{0.0351} = \ln t + 16.30 \quad (1400\ ^\circ\text{C}) \quad (30)$$

$$\frac{Q^2_{od}}{0.0363} = \ln t + 15.23 \quad (1300\ ^\circ\text{C}) \quad (31)$$

$$\frac{Q^2_{od}}{0.0434} = \ln t + 11.24 \quad (1200\ ^\circ\text{C}) \quad (32)$$

$$\frac{Q^2_{od}}{0.0455} = \ln t + 8.55 \quad (1100\ ^\circ\text{C}). \quad (33)$$

By comparison with Equation 26, a plot of the right hand side of Equations 30–33 at ln t = 0 against $1/T$ will give ΔH^* from the slope and $(\Delta S^*/R - \ln \tau_0)$ from the intercept. Values of 124 ± ~15 kcal/mol and 54.3 have been obtained for these terms from a least-squares analysis of the data shown in Figure 12. Similarly, values of the denominator on the left hand side of Equations 30–33 give T_c = 2215 °C and $A = -2.1 \times 10^{-5}$.

The observed activation energy is comparable to activation energies obtained for Al-Si diffusion in calcic plagioclase (123 ± 5 kcal/mol, Grove et al., 1984) for the incommensurate → commensurate ordering transition in anorthite (135 ± 14 kcal/mol, Carpenter, 1991a) and for APD coarsening in anorthite (between 121 and 152 kcal/mol, Carpenter, 1991a). The parameters ΔS^* and τ_0 cannot be separated with the present data, but expressed in units of time, $\tau_0 \exp(-\Delta S^*/R)$ is 9×10^{-21} s and may be compared with 9×10^{-19} s for an equivalent term for Mg-Al-Na-Ca disordering in omphacite (Carpenter et al., 1990b). It combines a frequency factor and entropy of activation, as is the case in many phenomenological rate equations requiring movement of atoms between crystallographic sites. The physical origin of the proportionality constant, A, is not clear, but in the kinetic analysis of Salje (1988) it is related to a probability distribution for values of local order parameter susceptibilities in crystals that are inhomogeneous with respect to their local degrees of order (see following section).

Theoretical framework: the Ginzburg-Landau rate equation

A theoretical basis for understanding the variation of a macroscopic order parameter, Q, with time, t, in a kinetic experiment is provided by the Ginzburg-Landau (GL) equation:

$$\frac{dQ}{dt} = \frac{-\gamma\lambda \exp(-\Delta G^*/RT)}{2RT} \frac{\partial G}{\partial Q} \quad (34)$$

where γ and λ are material constants and ΔG^* is the free energy of activation. As discussed at length by Salje (1988) and Carpenter and Salje (1989), the GL equation applies strictly only to systems in which the correlation length of Q is large relative to the length scale of conservation, a condition which appears to be obeyed in the case of order-disorder processes in framework silicates. Many specific solutions to this general rate law exist, depending on the form of the free energy dependence on Q and the form of any dependence of ΔG^* on Q. Exact or numerical so-

lutions may be obtained if such relationships can be expressed explicitly and if values for the various coefficients are known. A description of the ordering or disordering process from the start time, t_0, to the finish time, t, is then given by integration over $t_0 \rightarrow t$. An analysis of this type has been achieved for cation disordering in omphacite, where Q remains homogeneous on the length scale of X-ray diffraction (Carpenter et al., 1990b). In anorthite, the Al-Si ordering process gives rise to local inhomogeneities in Q_{od}, however, and the coefficients describing the thermodynamic driving force are not known. Only partial solutions for limited ranges of t and Q_{od} can therefore be obtained at present, but these nevertheless indicate the underlying physical constraints on the kinetics.

In the simplest solution to the GL equation, the equilibrium phase transition is treated as second order and Q is assumed to remain homogeneous throughout a given crystal of interest. The free energy variation with Q at some temperature below T_c would then show the usual minimum at the equilibrium value of Q, Q_{eqm}, as illustrated in Figure 8. For a crystal with some degree of order, Q', the total driving force for ordering toward Q_{eqm} is ΔG (Fig. 8). The dependence of ΔG upon ΔQ ($= Q' - Q_{eqm}$) is expressed in the harmonic approximation as

$$\Delta G = \chi^{-1} \cdot \Delta Q \tag{35}$$

where χ is the order parameter susceptibility, i.e., the curvature of the free energy curve $[\partial^2(\Delta G)/\partial(\Delta Q)^2 = \chi^{-1}$, with χ^{-1} treated as a constant at the temperature of the kinetic experiment]. Salje (1988) showed that this leads to a rate law of the form

$$\ln(\Delta Q) \propto t. \tag{36}$$

In a crystal that does not remain homogeneous with respect to local values of Q, the average macroscopic order parameter, $\langle Q \rangle$, will follow a different rate law depending on how the individual regions evolve. The problem becomes one of determining a local rate law and then integrating over all local regions. Salje and Wruck (1988) showed that if individual homogeneous regions follow Equation 36, this integration procedure can be expressed as

$$\langle Q \rangle = \mathrm{L}(P) = \int_0^\infty P(\chi_{\mathrm{eff}}^{-1}) \mathrm{e}^{-\chi_{\mathrm{eff}}^{-1} t} \cdot \mathrm{d}\chi_{\mathrm{eff}}^{-1} \tag{37}$$

where L is the Laplace transformation. $P(\chi_{\mathrm{eff}}^{-1})$ now represents a probability distribution for different values of the effective local susceptibilities, χ_{eff}^{-1}. In other words, each local region has its own susceptibility given by

$$\chi_{\mathrm{eff}}^{-1} = \chi^{-1} + \chi_r^{-1} \tag{38}$$

where χ_r^{-1} describes the contribution of inhomogeneities in Q (or indeed, of any other defects) to the local free energy variation with Q. Different probability distributions give differing rate laws, and the nearest appropriate function that has so far been evaluated has

$$\lim_{\chi_{\mathrm{eff}}^{-1} \rightarrow 0} P(\chi_{\mathrm{eff}}^{-1}) = (\chi_{\mathrm{eff}}^{-1})^{-1} \tag{39}$$

and gives (from Salje and Wruck, 1988)

$$\langle Q \rangle \propto \ln t. \tag{40}$$

Although this is not quite the observed rate law, some related distribution of $P(\chi_{\mathrm{eff}}^{-1})$ may be appropriate. The physical insight suggested by Equation 39 would be that a relatively large number of local regions have rather flat free energy variations with Q (small χ_{eff}^{-1}). The contribution, χ_r^{-1}, of local inhomogeneities thus appears to have opposite sign from χ^{-1} for a homogeneous crystal, i.e., the inhomogeneities in Q around a local region have the effect of reducing the free energy driving force for ordering in that region.

An alternative approach to defining the effect of inhomogeneities in Q arises from a mean-field model (Salje, 1988; Carpenter and Salje, 1989). The main idea is again that the energetics and, hence, kinetics of ordering in one region of crystal are influenced by the configuration of neighboring regions. In a homogeneous crystal, this influence, or local "field," is uniform and corresponds to some mean field. In an inhomogeneous crystal, the local fields are different, and if their distribution has a sufficiently broad Gaussian form, the $Q^2 \propto \ln t$ rate law results from integration over the mesoscopic regions.

A third approach is to assume that the activation energy is sensitive to Q. For cation disordering in omphacite, $Q^2 \propto \ln t$ behavior has been explained by setting

$$\Delta G^* = \Delta H^* - T(\Delta S^* + \varphi Q^2) \tag{41}$$

where φ is a constant (Carpenter et al., 1990b). The effective entropy of activation is $\Delta S^* + \varphi Q^2$, and a physical interpretation is that the proportion of all possible activated states that can lead to a change of Q in the desired direction depends on the local configuration of atoms and hence on the local degree of order. The value of ΔH^* might also depend on Q if the energy of Al-O and Si-O bonds varies significantly with the distribution of second-nearest neighbor atoms but the effect is likely to be much less marked.

The common factor in these three physical pictures of the ordering sequence is that variations in the degree of local order in a crystal will modify the evolution of each small local region. The effect can be expressed as a probability distribution of mesoscopic domains with differing order parameter susceptibilities, a variation in local effective fields or a configurational dependence of the activation energy. In reality, the alternative approaches may only be providing differing mathematical descriptions of the same fundamental process. They all emphasize the importance of mesoscopic scale interactions, i.e., on a scale of more than a few unit cells, on the observed macroscopic behavior, however.

Discussion and conclusions

Al-Si ordering in anorthite under nonequilibrium conditions results in a rather well-defined sequence of structural states. The initially disordered or short-range ordered crystals grown from glass evolve through an

incommensurate structure to the stable commensurate structure in an apparently continuous manner. The combined calorimetric and strain data presented here for a suite of crystals with metastable intermediate states provide some new insights into the energetics and mechanisms of ordering on three different length scales.

At a microscopic, i.e., atomic, scale it is clear from the characteristic activation energy of ~130 kcal/mol that individual Al-Si exchanges are involved in the rate determining step, whether the particular process of interest is APD coarsening, order parameter evolution, or the incommensurate → commensurate transition. On a mesoscopic scale, however, each of these processes involves a quite different mechanism. During APD coarsening, cooperative Al-Si exchanges are required along the length of the APBs, which then move with a velocity that depends on their curvature (Allen and Cahn, 1979). Changes of Q_{od} also require cooperative Al-Si exchanges in a finite volume of crystal. The evolution of an individual region a few unit cells across is sensitive to the configuration in neighboring regions, but in this case, the driving forces may be analyzed in terms of the order parameter susceptibilities of the local mesoscopic regions. A correlation length scale of at least a few hundred ångstroms is suggested by the development of the IC structure in which initial inhomogeneities in Q_{od}^{1} are amplified by gradient coupling with a second order parameter, suggested to be Q_{od}^{2}. The modulations have a well-defined wavelength and orientation, and their rotation or coarsening requires further correlated Al-Si exchanges over at least the same length scale., Finally, the macroscopic evolution of the anorthite crystals clearly depends both on the mechanism of individual Al-Si exchanges and on the nature of interactions between the mesoscopic regions.

Any interaction mechanism that allows correlations on such different length scales is unlikely to be purely ionic. As has been discussed by Carpenter (1988), framework silicate structures are in effect three dimensional linkages of only semiflexible Al-O-Al, Si-O-Al, and Si-O-Si bonds. Changes in the occupancy at one tetrahedral site produce a local distortion as the bond angles adjust to their new minimum energy values. This distortion is transmitted through the structure as a strain field by further bond angle adjustments for distances of up to at least ~0.1 μm (Carpenter, 1988). The picture that emerges is of continuous exchanges between adjacent Al and Si atoms, with a net drift of the average site occupancies toward lower free energy states and along particular reaction pathways that are strongly influenced by strain effects. Al-Si ordering in cordierite appears to be somewhat analogous since, under nonequilibrium conditions, the sequence of structural states also involves a metastable modulated phase. There is a distinct discontinuity between the modulated state and stable orthorhombic cordierite, however (Putnis et al., 1987).

In conclusion, the use of a macroscopic order parameter as the common parameter in both equilibrium and kinetic experiments utilizes the interdependence of equilibrium driving forces and nonequilibrium reaction pathways. The equilibrium behavior may be easier to predict in many systems because of the uniqueness of states defined by minima in G, but kinetic behavior is certainly not random. Although an infinite number of reaction pathways may exist in principle, the actual pathway followed will tend to make use of related structural states that may even have stability fields at other pressures, temperatures, or compositions. The GL equation provides a formal basis for linking these different states and should also provide a means of rationalizing the evolution of minerals in nature when nonequilibrium conditions prevail.

Acknowledgments

This paper provides a timely opportunity for the author to thank A. Navrotsky for her generous assistance and encouragement in setting up the Cambridge solution calorimeter facility. Discussions with E. Salje have, as usual, led to significant improvements in the thermodynamic and kinetic analysis. The computer program to calculate strains from lattice parameter data was written by S.A.T. Redfern. R.J. Angel and J. Boerio-Goates are thanked for their critical reviews of the manuscript, which led to a number of improvements. Support from the Nuffield Foundation, in the form of a Science Research Fellowship, and from the Natural Environment Research Council of Great Britain (grant no. GR3/5547) is also gratefully acknowledged. This paper is Cambridge Earth Sciences contribution no. 1812.

References cited

Allen, S.M., and Cahn, J.W. (1979) A microscopic theory for antiphase boundary motion and its application to antiphase domain coarsening. Acta Metallurgica, 27, 1085–1095.

Becker, R. (1978) Theorie der Wärme, 336 p. Springer-Verlag, Berlin.

Borg, I.Y., and Smith, D.K. (1969) Calculated X-ray powder patterns for silicate minerals. Geological Society of America Memoir, 122, 896 p.

Burnham, C.W. (1962) Lattice constant refinement. Carnegie Institution of Washington Year Book, 61, 132–135.

Carpenter, M.A. (1988) Thermochemistry of aluminium/silicon ordering in feldspar minerals. In E.K.H. Salje, Ed., Physical properties and thermodynamic behaviour of minerals. NATO ASI series C, 225, p. 265–323. Reidel, Dordrecht.

——— (1991a) Mechanisms and kinetics of Al-Si ordering in anorthite: I. Incommensurate structure and domain coarsening. American Mineralogist, 76, 1110–1119.

——— (1991b) Thermodynamics of phase transitions in minerals: A macroscopic approach. In N.L. Ross and G.D. Price, Eds., Stability of minerals. Unwin Hayman, London.

Carpenter, M.A., and Salje, E. (1989) Time-dependent Landau theory for order/disorder processes in minerals. Mineralogical Magazine, 53, 483–504.

Carpenter, M.A., Putnis, A., Navrotsky, A., and McConnell, J.D.C. (1983) Enthalpy effects associated with Al/Si ordering in anhydrous Mg-cordierite. Geochimica et Cosmochimica Acta, 47, 899–906.

Carpenter, M.A., McConnell, J.D.C., and Navrotsky, A. (1985) Enthalpies of ordering in the plagioclase feldspar solid solution. Geochimica et Cosmochimica Acta, 49, 947–966.

Carpenter, M.A., Domeneghetti, M.-C., and Tazzoli, V. (1990a) Application of Landau theory to cation ordering in omphacite I: Equilibrium behaviour. European Journal of Mineralogy, 2, 7–18.

——— (1990b) Application of Landau theory to cation ordering in omphacite II: Kinetic behaviour. European Journal of Mineralogy, 2, 19–28.

Carpenter, M.A., Angel, R.J., and Finger, L.W. (1990c) Calibration of Al/Si order variations in anorthite. Contributions to Mineralogy and Petrology, 104, 471–480.

Grove, T.L., Baker, M.B., and Kinzler, R.J. (1984) Coupled CaAl-NaSi

diffusion in plagioclase feldspar: Experiments and applications to cooling rate speedometry. Geochimica et Cosmochimica Acta, 48, 2113–2121.

Navrotsky, A. (1977) Progress and new directions in high temperature calorimetry. Physics and Chemistry of Minerals, 2, 89–104.

Nord, G.L., Jr., and Lawson, C.A. (1989) Order-disorder transition-induced twin domains and magnetic properties in ilmenite-hematite. American Mineralogist, 74, 160–176.

Putnis, A. (1988) Solid state NMR spectroscopy and phase transitions in minerals. In E.K.H. Salje, Ed., Physical properties and thermodynamic behaviour of minerals. NATO ASI series C, 225, p. 325–358. Reidel, Dordrecht.

Putnis, A., and Angel, R.J. (1985) Al, Si ordering in cordierite using "magic angle spinning" NMR. II: Models of Al, Si order from NMR data. Physics and Chemistry of Minerals, 12, 217–222.

Putnis, A., Fyfe, C.A., and Gobbi, G.C. (1985) Al, Si ordering in cordierite using "magic angle spinning" NMR. I. Si^{29} spectra of synthetic cordierites. Physics and Chemistry of Minerals, 12, 211–216.

Putnis, A., Salje, E., Redfern, S.A.T., Fyfe, C.A., and Strobl, H. (1987) Structural states of Mg-cordierite, I: Order parameters from synchrotron X-ray and NMR data. Physics and Chemistry of Minerals, 14, 446–454.

Redfern, S.A.T. (1989) The thermodynamics of displacive phase transitions in framework silicates. Ph.D. thesis, University of Cambridge, Cambridge, England.

Redfern, S.A.T., and Salje, E. (1987) Thermodynamics of plagioclase II: Temperature evolution of the spontaneous strain at the $I\bar{1} \leftrightarrow P\bar{1}$ phase transition in anorthite. Physics and Chemistry of Minerals, 14, 189–195.

Salje, E. (1987) Structural states of Mg-cordierite II: Landau theory. Physics and Chemistry of Minerals, 14, 455–460.

——— (1988) Kinetic rate laws as derived from order parameter theory I: Theoretical concepts. Physics and Chemistry of Minerals, 15, 336–348.

——— (1989) Towards a better understanding of time-dependent geological processes: Kinetics of structural phase transformations in minerals. Terra Nova, 1, 35–44.

Salje, E., and Wruck, B. (1988) Kinetic rate laws as derived from order parameter theory II: Interpretation of experimental data by Laplace-transformation, the relaxation spectrum, and kinetic gradient coupling between two order parameters. Physics and Chemistry of Minerals, 16, 140–147.

Salje, E., Kuscholke, B., Wruck, B., and Kroll, H. (1985) Thermodynamics of sodium feldspar II: Experimental results and numerical calculations. Physics and Chemistry of Minerals, 12, 99–107.

Smith, C.S., and Guttman, L. (1953) Measurement of internal boundaries in three-dimensional structures by random sectioning. Transactions of the Metallurgical Society of AIME, 197, 81–87.

Smith, J.V., and Brown, W.L. (1988) Feldspar minerals. I: Crystal structures, physical, chemical and microtextural properties (2nd edition), 828 p. Springer-Verlag, New York.

Manuscript received May 7, 1990
Manuscript accepted April 9, 1991